

ANL-HEP-PR-96-15

RAL-TR-96-057

July 1996

# Inclusive Prompt Photon Production in Polarized $pp$ Collisions at HERA- $\vec{N}$

L.E. Gordon

High Energy Physics Division, Argonne National Laboratory,  
Argonne IL 60439, USA

W. Vogelsang

Rutherford Appleton Laboratory,  
Chilton DIDCOT, Oxon OX11 0QX, England

## Abstract

We present a NLO study of inclusive polarized prompt photon production in a conceivable fixed target  $pp$  mode of HERA with longitudinally polarized protons at  $\sqrt{s} = 39$  GeV. We analyze the sensitivity of the corresponding double spin asymmetry to the proton's polarized gluon distribution  $\Delta g$  and estimate the expected statistical precision in its determination. The main theoretical uncertainties in the predictions are examined.

It has recently become possible to perform a complete and consistent study of longitudinally polarized deep-inelastic scattering (DIS) in next-to-leading order (NLO) of QCD, since the spin-dependent two-loop splitting functions, needed for the NLO evolution of the polarized parton distributions, have become available [1, 2]. A first such phenomenological NLO analysis, taking into account all available experimental data on polarized DIS [3] has been presented in [4], followed by the analyses [5, 6]. The studies of [4, 6] have shown that present polarized DIS data are still quite far from providing accurate knowledge about the nucleon's spin-dependent sea quark and gluon distributions. This holds true, in particular, for the polarized gluon density  $\Delta g$ , the  $x$ -shape of which seems to be hardly constrained at all [4, 6] by the DIS data, even though a tendency towards a sizeable positive *total* gluon polarization,  $\int_0^1 \Delta g(x, Q^2 = 4 \text{ GeV}^2) dx \gtrsim 1$ , was found [4, 5, 6]. Thus, there is clearly some need for independent information on  $\Delta g$ . For this purpose, it seems expedient to look at processes for which  $\Delta g$  enters in leading order (LO) already, rather than as a NLO correction as for the spin-dependent DIS structure function  $g_1$ . One of such processes is inclusive large- $p_T$  prompt photon production in collisions of longitudinally polarized protons,  $\vec{p}\vec{p} \rightarrow \gamma X$  [7, 8, 9, 10]. In the unpolarized case where this process has been studied in a huge number of experiments it has been an invaluable tool for pinning down the proton's unpolarized gluon distribution  $g(x, Q^2)$  [11, 12, 13, 14]. Hence prompt photon production with polarized beams seems a promising source for obtaining information on  $\Delta g$ .

It is being discussed as one future option for HERA to polarize its 820 GeV proton beam. If this can be achieved, one could use the beam in a fixed target experiment, scattering it off an internal polarized nucleon target. This conceivable constellation, dubbed 'Phase II' of HERA- $\vec{N}$  [15], would yield  $\sqrt{s} \approx 39 \text{ GeV}$  and thus could provide information complementary to that obtained from planned similar spin physics experiments at much higher energies at the RHIC collider [16]. Theoretical predictions for polarized prompt photon production at  $\sqrt{s} \approx 40 \text{ GeV}$  have been made in the past [8, 10], taking into account the spin-dependent 'direct' subprocess cross sections for  $ab \rightarrow \gamma X$  ( $a, b = q, \bar{q}, g$ ) including their full NLO QCD corrections as calculated in [8, 9]. From the experience in the unpolarized case, the inclusion of NLO corrections is expected to be quite important

in order to make reliable predictions. The main shortcoming of the studies [8, 10] was, however, that spin-dependent parton densities evolved only in LO had to be used at that time. Having sets of NLO polarized parton distributions available now, we can obviously put the corresponding predictions as well as the assessment of their theoretical uncertainties such as their scale dependence on a much firmer basis, which is the purpose of this paper. The only remaining drawback here is that the fragmentation contribution to the polarized prompt photon cross section still cannot be calculated in NLO since the NLO corrections to the underlying polarized subprocesses  $ab \rightarrow cX$  ( $a, b, c = q, \bar{q}, g$ ) are not yet known. On the other hand, in the unpolarized case the fragmentation piece is known to be subdominant – even though not negligible – at fixed target energies (see, e.g., [14]). The fragmentation contribution to the polarized cross section which was omitted altogether in [8, 10], will be included on a LO basis in this paper. Even though this is not strictly consistent in the framework of a NLO calculation, it is the best ‘state-of-the-art’ procedure and also appears reasonable in view of the fact that the  $K$ -factor  $K^{frag} \equiv \sigma_{NLO}^{frag}/\sigma_{LO}^{frag}$  for the fully inclusive fragmentation part generally turns out to be very close to unity when calculated for the unpolarized case.

The analyses of [4, 6] provide several different sets of LO and NLO spin-dependent parton densities, all of which are in very good agreement with the existing polarized DIS data but differ mainly in the  $x$ -shapes of their polarized gluon distributions. We are therefore in the position to study the sensitivity of polarized prompt photon production to  $\Delta g(x, Q^2)$  on the basis of consistent NLO sets of parton distributions that include all experimental information presently available from DIS, but also reflect the full freedom concerning  $\Delta g$  left by those data. The latter is illustrated in Fig. 1 which compares the gluon distributions of various NLO sets of [4, 6] in the  $x$ -range dominantly probed by prompt photon production at  $\sqrt{s} = 39$  GeV and  $p_T \geq 3$  GeV. The sets we will use in our study are the NLO ‘valence’ set of the ‘radiative parton model analysis’ [4], which corresponds to the best-fit result of that paper (hereafter referred to as ‘fitted  $\Delta g$ ’ scenario), and two other sets of [4] which are based on either assuming  $\Delta g(x, \mu^2) = g(x, \mu^2)$  or  $\Delta g(x, \mu^2) = 0$  at the low input scale  $\mu$  of [4], where  $g(x, \mu^2)$  is the unpolarized NLO GRV [17] input gluon distribution. These two sets will be called ‘ $\Delta g = g$  input’ and

' $\Delta g = 0$  input' scenarios, respectively, in what follows. It turns out that in the  $x$ -range explored here the NLO sets A,B of [6] have gluon distributions quite similar to those of the ' $\Delta g = g$  input' and 'fitted  $\Delta g$ ' scenarios of [4], respectively. Only the gluon of set C of [6] ('GS C') is qualitatively different since it has a substantial negative polarization at large  $x$ . We will therefore also use this set in our calculations. A graph similar to Fig. 1 could be shown for the corresponding LO gluon distributions of [4, 6] (see, e.g., [18]). The fact that [4, 6] have provided both consistent LO *and* NLO parton sets in all cases, enables us to more reliably study the perturbative stability of the cross sections and asymmetries. This is again a major improvement with respect to the previous studies [8, 10].

The quantity to be studied in prompt photon experiments with polarized beam and target is the double-spin asymmetry

$$A_{LL} \equiv \frac{d\sigma^{++} - d\sigma^{+-}}{d\sigma^{++} + d\sigma^{+-}} \equiv \frac{d\Delta\sigma}{d\sigma}, \quad (1)$$

where  $d\sigma^{++}$  ( $d\sigma^{+-}$ ) denotes the cross section for the prompt photon being produced by protons with same (opposite) helicities. Two types of processes contribute to the prompt photon production cross section: the so-called 'direct' piece, where the photon is emitted via a pointlike (direct) coupling to a quark, and the fragmentation piece, in which the photon originates from the fragmentation of a final state parton. The cross section for the fully inclusive production of a prompt photon with momentum  $p_\gamma$  thus schematically reads

$$\begin{aligned} d\Delta\sigma &\equiv \frac{1}{2} (d\sigma^{++} - d\sigma^{+-}) \equiv d\Delta\sigma_{dir} + d\Delta\sigma_{frag} \\ &= \sum_{a,b=q,\bar{q},g} \int dx_a dx_b \Delta f_a(x_a, \mu_F^2) \Delta f_b(x_b, \mu_F^2) \left[ d\Delta\sigma_{ab}^\gamma(p_\gamma, x_a, x_b, \mu_R, \mu_F, M_F) \right. \\ &\quad \left. + \sum_{c=q,\bar{q},g} \int \frac{dz}{z^2} d\Delta\sigma_{ab}^c(p_\gamma, x_a, x_b, z, \mu_R, \mu_F, M_F) D_c^\gamma(z, M_F^2) \right], \end{aligned} \quad (2)$$

where the  $d\Delta\sigma_{ab}^i$  represent the spin-dependent subprocess cross sections for partons  $a, b$  producing a particle  $i$  ( $i = \gamma, q, \bar{q}, g$ ), integrated over the full phase space of all other final state particles. The polarized parton distributions are defined as

$$\Delta f_i(x, \mu_F^2) = f_i^+(x, \mu_F^2) - f_i^-(x, \mu_F^2), \quad (3)$$

with  $f_i^+(x, \mu_F^2)$  ( $f_i^-(x, \mu_F^2)$ ) denoting the number density of parton-type  $i$  with momentum fraction  $x$  and positive (negative) helicity in a proton with positive helicity at scale  $\mu_F$ . Furthermore, in (2)  $D_c^\gamma(z, M_F^2)$  is the (unpolarized) photon fragmentation function at scale  $M_F$ ,  $z$  being the fraction of energy of the fragmenting parton  $c$  transferred to the photon. We note that even in the polarized case the photon fragmentation functions are always the unpolarized ones since the polarization of the outgoing photon is not observed. Despite the fact that its corresponding partonic subprocesses are of order  $\alpha_s^2$ , the fragmentation contribution is present already in LO since the parton-to-photon fragmentation functions are effectively of order  $\alpha_{e.m.}/\alpha_s$  in perturbative QCD. As made explicit in (2), the cross section in any fixed order of perturbation theory depends on unphysical scales which have to be introduced in the procedure of renormalization ( $\mu_R$ ) and of factorization of initial ( $\mu_F$ ) and final ( $M_F$ ) state mass singularities. Unless stated otherwise, we will choose  $\mu_R = \mu_F = M_F = p_T/2$  in what follows.

The corresponding expressions for the unpolarized cross section, which we need to calculate the spin asymmetry  $A_{LL}$ , can be obtained from (2),(3) by omitting the ' $\Delta$ ' and taking sums instead of the differences on the rhs. In this case, all cross sections  $d\sigma_{ab}^i$  ( $i = \gamma, q, \bar{q}, g$ ) are known to NLO accuracy, the corrections to the direct and fragmentation subprocess cross sections having been calculated in the  $\overline{\text{MS}}$  scheme in [19, 9] and [20], respectively. For consistency, when including these NLO corrections, we have to use NLO unpolarized parton densities and photon fragmentation functions. For the latter we use those of GRV [21] throughout. The specific choice for the protonic parton densities turns out to be rather immaterial, all modern parametrizations leading to essentially the same results. The sets of spin-dependent NLO parton densities we want to use have in each case been set up in relation to some underlying 'reference' set of NLO *unpolarized* densities: For the distributions of [4] this has been the GRV set [17], whereas the MRS(A') densities [12] have been adopted in [6]. For definiteness, we will choose the GRV NLO parton distributions [17] as our 'standard' for the unpolarized case, but use the MRS(A') set [12] when employing the polarized NLO densities of [6]. This also implies using the values for  $\Lambda_{\overline{\text{MS}}}^{(f)}$  ( $f$  being the number of flavors) as implemented in the respective NLO sets, e.g.  $\Lambda_{\overline{\text{MS}}}^{(f=4)} = 200$  MeV for the GRV and  $\Lambda_{\overline{\text{MS}}}^{(f=4)} = 231$  MeV for the MRS(A') set, in the NLO

expression for the strong coupling  $\alpha_s$ :

$$\frac{\alpha_s(Q^2)}{4\pi} \simeq \frac{1}{\beta_0 \ln Q^2/\Lambda_{\overline{\text{MS}}}^2} - \frac{\beta_1}{\beta_0^3} \frac{\ln \ln Q^2/\Lambda_{\overline{\text{MS}}}^2}{\left(\ln Q^2/\Lambda_{\overline{\text{MS}}}^2\right)^2}, \quad (4)$$

where  $\beta_0 = 11 - 2f/3$ ,  $\beta_1 = 102 - 38f/3$ . As provided for in the sets of [17, 12], the number of flavors increases when crossing a heavy flavor threshold, and the value for  $\Lambda_{\overline{\text{MS}}}^{(f)}$  changes as a result of the continuity of  $\alpha_s$  across the threshold. We follow this prescription also for the explicit  $f$  appearing in the NLO subprocess cross sections. We neglect, however, the genuine charm (and, of course, bottom) contributions to the polarized and unpolarized cross sections which are tiny at  $\sqrt{s} = 39$  GeV [14].

In the polarized case, next-to-leading order QCD corrections have been calculated for the spin-dependent direct subprocess cross sections  $d\Delta\sigma_{ab}^\gamma$  [8, 9]. We emphasize that care has to be taken when combining the NLO sets of polarized parton distributions of [4, 6] with the NLO expressions for the  $d\Delta\sigma_{ab}^\gamma$  of [8, 9] to avoid a mismatch in the factorization schemes used. The two-loop splitting functions of [1, 2], which were employed in [4, 6], have been calculated in dimensional regularization in the conventional  $\overline{\text{MS}}$  scheme. To be more precise, use of dimensional regularization in such a calculation implies to choose a prescription for dealing with the Dirac matrix  $\gamma_5$  and the Levi-Civita tensor  $\epsilon_{\mu\nu\rho\sigma}$  which enter as projectors onto definite helicity states of the involved particles. In [1] the 'reading point' method of [22] with a fully anticommuting  $\gamma_5$  was chosen, whereas [2] adopted the original definition for  $\gamma_5$  of [23] (HVBM scheme) which is widely considered to be the most consistent prescription. It turned out that both calculations [1, 2] arrived at the same final result for the polarized two-loop splitting functions. The polarized NLO parton distributions of [4, 6] therefore refer to the conventional  $\overline{\text{MS}}$  factorization scheme *in combination* with the HVBM prescription [23] (or the one of [22]) for  $\gamma_5$ , and the NLO  $d\Delta\sigma_{ab}^\gamma$  have to be known in the *same* scheme to make it sensible to use them in conjunction with the NLO partons of [4, 6]. In fact, the calculation of [9] of the NLO corrections to the  $d\Delta\sigma_{ab}^\gamma$  has been performed using the HVBM prescription, which makes the results suitable for our purposes. We note, however, that in [9] a slight deviation from the  $\overline{\text{MS}}$  scheme was made by factorizing certain finite 'collinear' terms, arising from the non-fourdimensional parts of the polarized LO splitting functions as calculated in the

HVBM scheme, into the NLO spin-dependent parton densities along with the collinear singularities (' $\overline{\text{MS}}_P$  scheme'). It is straightforward to invert this procedure, i.e., to bring back the results of [9] to the conventional  $\overline{\text{MS}}$  scheme. Details of this are given in the appendix. We note that we refrain from using the results of [8] for the NLO corrections to the  $d\Delta\sigma_{ab}^\gamma$  since it is not obvious whether the  $\gamma_5$  scheme used in [8] provides a consistent regularization and can be related in any way to the HVBM prescription.

Unfortunately, the NLO corrections to the polarized fragmentation subprocess cross sections  $d\Delta\sigma_{ab}^i$  ( $i = q, \bar{q}, g$ ) are still unknown as mentioned above. For this reason we stick to a pure LO calculation for this contribution, using the corresponding spin-dependent LO subprocess cross sections of [24] along with the respective LO sets of polarized parton distributions of [4, 6], and the LO expression for  $\alpha_s$  (as entailed in (4) by dropping the  $\beta_1$  term) with [17]  $\Lambda_{LO}^{(f=4)} = 200$  MeV. For the photon fragmentation functions we use the LO set of [21] in this case.

Fig. 2a shows the NLO predictions for the spin-dependent cross sections  $d\Delta\sigma/dp_T d\eta$  as functions of the prompt photon's transverse momentum  $p_T$  at c.m.s. rapidity  $\eta = 0$  for the four different sets of polarized parton distributions. We also display the unpolarized NLO cross section. In Fig. 2b we show the asymmetries  $A_{LL}$  corresponding to Fig. 2a. As becomes obvious,  $A_{LL}$  depends strongly on the size and shape of  $\Delta g$  even at large  $p_T$ . When artificially setting  $\Delta g(x, \mu_F^2) \equiv 0$  one finds that the asymmetry becomes very small and negative for all  $p_T$  and all four sets of polarized parton distributions. Thus the differences between the results in Fig. 2b are indeed due to the polarized gluon distribution employed. The small negative 'offset' in the asymmetry obtained for  $\Delta g(x, \mu_F^2) \equiv 0$  turns out to be due to the LO annihilation process  $q\bar{q} \rightarrow \gamma g$  and NLO corrections involving only incoming quarks and is mainly responsible for the fact that the asymmetries for the ' $\Delta g = 0$  input' and the 'fitted  $\Delta g$ ' scenarios of [4] are much closer to each other at large  $p_T$  than those for the 'fitted  $\Delta g$ ' and the ' $\Delta g = g$  input' scenarios. We also note that the full (LO) fragmentation contribution to the polarized cross section is positive for all parton sets (apart from set C of [6] at small to medium  $p_T$ ) and not very sensitive to  $\Delta g$  for  $p_T \gtrsim 7$  GeV.

Figs. 2b,d show the same quantities as Figs. 2a,c, but now as functions of  $\eta$  at  $p_T = 6$  GeV. We note that the rapidity range  $-1.5 \leq \eta \leq 1.5$  shown is equivalent to laboratory angles of  $0.9^\circ \leq \Theta_{lab} \leq 17^\circ$ , which roughly corresponds to the range expected to be accessible in the HERA- $\vec{N}$  experiment at this  $p_T$  [15]. Again, the asymmetries in Fig. 2d show strong sensitivity to  $\Delta g$ , even becoming slightly better at large  $|\eta|$ .

We have included in the asymmetry plots in Figs. 2b,d the expected statistical errors  $\delta A_{LL}$  at HERA- $\vec{N}$  which can be estimated from

$$\delta A_{LL} = 0.17 / \sqrt{\sigma \text{ (pb)}} . \quad (5)$$

This relation has been determined in [15] assuming an integrated luminosity of  $240 \text{ pb}^{-1}$  and beam and target polarizations  $P_B = 0.6$ ,  $P_T = 0.8$ . It includes an overall trigger and reconstruction efficiency of 50% but no acceptance correction. The error bars in Figs. 2b,d have been obtained using our unpolarized NLO  $d\sigma/dp_T d\eta$  in (5), integrated over bins of  $\Delta\eta = 1$ ,  $\Delta p_T = 1$  GeV. The bars have been plotted at the weighted centers of the bins. It becomes obvious that the asymmetry should be measurable by HERA- $\vec{N}$  for  $p_T \leq 7$  GeV and for almost all accessible  $\eta$ , and one should be able to distinguish between different scenarios for  $\Delta g(x, \mu_F^2)$  at  $0.1 \leq x \leq 0.4$ .

The remainder of this paper is devoted to an examination of the reliability of the predictions of these very positive findings. We will first discuss the actual size of the NLO effects that we have included, and then try to assess the main uncertainties in the predictions.

Figs. 3a,c show the  $K$ -factors

$$K \equiv \frac{d(\Delta)\sigma_{NLO}}{d(\Delta)\sigma_{LO}} \quad (6)$$

for the unpolarized and the polarized cross sections for our three sets of spin-dependent parton distributions of [4]. From now on, we do not show the corresponding results for set C of [6] to avoid a proliferation of curves. For the  $K$ -factors the LO cross sections in (6) have been calculated consistently, i.e. with LO parton distributions and photon fragmentation functions and LO  $\alpha_s$ . The  $K$ -factors turn out to be quite close to unity in

the experimentally accessible ranges of  $p_T$  and  $\eta$ . Only for the ' $\Delta g = 0$  input' scenario is the  $K$ -factor much less than unity around  $\eta = 0$  for all  $p_T$ , indicating rather significant NLO corrections in this case. Figs. 3b,d compare the asymmetries  $A_{LL}$  in NLO (as already shown in Figs. 2b,d) and LO. By comparison of Figs. 3a,c and 3b,d it can be seen that the asymmetries are to some extent less influenced by the NLO corrections than the individual polarized and unpolarized cross sections. This is again not true for the ' $\Delta g = 0$  input' scenario in Fig. 3b, whose asymmetry changes quite a lot for all  $p_T$  when going from LO to NLO. This feature for a scenario with a small  $\Delta g$  was already observed in [8, 10] and is due to sizeable negative contributions from direct genuine NLO processes like  $qq' \rightarrow \gamma qq'$ .

One major uncertainty in our predictions is expected to come from the fragmentation contribution since the parton-to-photon fragmentation functions are experimentally unmeasured so far, even though very sensible theoretical predictions for them are available [21, 25] (see also [14]). In our case, the uncertainty is even larger since, as discussed earlier, we have to stick to a pure LO calculation for the fragmentation contribution in the polarized case, rather than including it on a NLO basis as would be required by consistency. It seems likely, however, that the individual  $K$ -factor for fully inclusive polarized fragmentation is close to unity, just as it turns out to be in the unpolarized case<sup>1</sup>. Further investigation of this issue is needed in future, requiring a calculation of the NLO QCD corrections to the spin-dependent parton-parton scattering cross sections. To assess the importance of fragmentation, we show in Figs. 4a,c the ratios

$$R \equiv \frac{d(\Delta)\sigma_{frag}}{d(\Delta)\sigma_{dir} + d(\Delta)\sigma_{frag}} \quad (7)$$

in NLO (apart, of course, from the polarized  $d\Delta\sigma_{frag}$  which is LO). It turns out that the fragmentation contribution is generally of  $\mathcal{O}(20\%)$  at  $\sqrt{s} = 39$  GeV and in the ranges of  $p_T$ ,  $\eta$  shown (see also [14] for the unpolarized case), but that it is relatively much larger for the ' $\Delta g = 0$  input' scenario around  $\eta = 0$ , where its importance even rises with rising  $p_T$ . This surprising result is, however, in accord with our previous finding that the

---

<sup>1</sup>We note that this is no longer the case if the fragmentation contribution to the *isolated* prompt photon cross section, as measured at very high-energy colliders, is considered. Here the unpolarized fragmentation piece turns out to be substantially larger at NLO than when calculated in LO [26, 27]. This feature could set a limitation to the accuracy of similar theoretical predictions for polarized prompt photon production at RHIC where the introduction of some experimental isolation criterion will almost certainly be necessary.

fragmentation part is positive and rather independent of  $\Delta g$  at large  $p_T$ . Thus in the ' $\Delta g = 0$  input' scenario, where the direct contribution to the cross section is mainly due to the small and negative  $q\bar{q} \rightarrow \gamma g$  annihilation process, fragmentation plays an important role even at large  $p_T$  since cancellations between the direct and the fragmentation pieces occur. Even though it does not seem likely that the finding of general smallness of the asymmetry  $A_{LL}$  for this scenario would become invalid if fragmentation could be included at NLO, it means that our predictions for the ' $\Delta g = 0$  input' scenario are the least certain ones since a strong deviation of the individual  $K$ -factor for polarized fragmentation from unity would affect the predictions for this scenario most.

On the other hand, we find a very reassuring result in this context when examining another major source of uncertainty, namely the dependence of the results on the unphysical scales  $\mu_R$ ,  $\mu_F$  and  $M_F$ . It turns out that the dependence of *all* polarized cross sections on the fragmentation scale  $M_F$  alone is already *extremely* weak, even though fragmentation is only included in LO. This feature, which was also found in [14] for the fully inclusive unpolarized cross section (where NLO fragmentation was used) might be evidence for indeed very mild NLO corrections to polarized fragmentation.

In contrast to this, the dependence of the polarized and unpolarized NLO cross sections on the renormalization and initial-state factorization scales is very strong. For instance, changing the scales to  $\mu_R = \mu_F = M_F = 2p_T$  (we include the change of  $M_F$  here even though it has hardly any influence), the unpolarized NLO cross section decreases by  $\gtrsim 50\%$  almost uniformly over the whole ranges of  $p_T$  and  $\eta$  (see [14] for a closer examination of the notorious scale dependence of the unpolarized inclusive prompt photon cross section). Nevertheless, the asymmetries  $A_{LL}$ , which will be the quantities actually measured, remain quite untouched by scale changes, as can be seen from Figs. 4b,d. This finding is very important since it warrants the genuine sensitivity of  $A_{LL}$  to  $\Delta g$ , implying that despite the sizeable scale dependence of the cross sections it still seems a reasonable and safe procedure to compare theoretical predictions for the asymmetry with future data and to extract  $\Delta g$  from such comparisons.

In conclusion, we have presented a careful NLO analysis of HERA-N $\vec{N}$ 's capability

to measure the nucleon's polarized gluon distribution  $\Delta g$  in inclusive prompt photon production with polarized beam and target. The corresponding double spin asymmetry  $A_{LL}$  shows strong sensitivity to  $\Delta g$ , and its measurement as well as a distinction between various possible scenarios for  $\Delta g(x, \mu_F^2)$  in the range  $0.1 \leq x \leq 0.4$  should be possible experimentally. We have also assessed the uncertainties in the theoretical predictions for  $A_{LL}$  which appear to be under control.

## Acknowledgements

We are thankful to W.-D. Nowak for helpful comments. This work was supported in part by the US Department of Energy, Division of High Energy Physics, Contract number W-31-109-ENG-38.

## Appendix

In this appendix we list the changes in the NLO corrections to the direct part of polarized prompt photon production which are to be made to transform the results of [9] from the ' $\overline{\text{MS}}_P$  scheme' back to the conventional  $\overline{\text{MS}}$  scheme. They are entirely due to terms  $\sim \epsilon(1-x)$  in the polarized  $n = 4 - 2\epsilon$  dimensional LO splitting functions  $\Delta P_{ij}^{(n)}(x)$  ( $i, j = q, g$ ) as calculated in the HVBM scheme, which were absorbed into the spin-dependent parton densities in [9]. We emphasize that we must *not* undo this procedure of [9] for the case of  $\Delta P_{qq}^{(n)}(x)$  since in this case the subtraction of the adjacent terms  $\sim \epsilon(1-x)$  has also been performed in the calculation of the spin-dependent NLO splitting functions where it is demanded by the conservation of the axial non-singlet current [1, 2]. We therefore only have to reintroduce the effects of the terms  $\sim \epsilon(1-x)$  in  $\Delta P_{ij}^{(n)}(x)$  ( $\{ij\} \neq \{qq\}$ ) (as listed in [9]) into the polarized NLO cross sections. As a consequence of this, only the NLO cross sections for some subprocesses need to be changed. Furthermore only the coefficients  $\Delta c_{13}$  of [9], corresponding to the terms involving no logarithms and no distributions, are affected. The following terms have to be *added* to the coefficients

$\Delta_{c_{13}}$  in [9] to transform the corresponding polarized NLO subprocess cross sections back to the conventional  $\overline{\text{MS}}$  scheme:

$qg \rightarrow \gamma qg :$

$$-\frac{v^2(1-w)}{X^2} \left( 2(1+X)v^2w^2 + \frac{C_F}{N_C}(1-2Xvw) \right)$$

$gg \rightarrow \gamma q\bar{q} :$

$$\frac{1}{N_C}(2+Y)v^2(1-w)$$

$qq \rightarrow \gamma qq :$

$$\frac{C_F}{N_C X^2}(1-w) \left( (1-2X)(1+v)v_1^2 - v^2(Xv^2 + v^3 + v_1)w^2 \right)$$

$q\bar{q} \rightarrow \gamma q\bar{q} :$

$$\frac{C_F}{N_C X^2}(1-w) \left( (1-2X)(1+v)v_1^2 - v^2(Xv^2 + v^3 + v_1)w^2 \right)$$

$qq' \rightarrow \gamma qq' :$

$$-e_q^2 \frac{C_F}{N_C X^2}(1+X)v^4(1-w)w^2 - e_q'^2 \frac{C_F}{N_C}(1+v)v_1^2(1-w) ,$$

where  $C_F = 4/3$ ,  $N_C = 3$  and the variables  $v$ ,  $v_1$ ,  $w$ ,  $X$ ,  $Y$  are as defined in [9]. For the last process,  $e_q$  and  $e_q'$  denote the charges of  $q$  and  $q'$ , respectively. The coefficients  $\Delta_{c_{13}}$  for the processes  $q\bar{q} \rightarrow \gamma gg$  and  $q\bar{q} \rightarrow \gamma q'\bar{q}'$  remain unchanged.

## References

- [1] R. Mertig and W.L. van Neerven, Z. Phys. **C70** (1996) 637.
- [2] W. Vogelsang, Rutherford RAL-TR-95-071, to appear in Phys. Rev. **D**, and RAL-TR-96-020, to appear in Nucl. Phys. **B**.
- [3] A recent overview of the experimental status can be found, e.g., in R. Voss, in proceedings of the workshop on 'Deep Inelastic Scattering and QCD (DIS '95)', Paris, 1995, eds. J.F. Laporte and Y. Sirois.
- [4] M. Glück, E. Reya, M. Stratmann, and W. Vogelsang, Phys. Rev. **D53** (1996) 4775.

- [5] R.D. Ball, S. Forte, and G. Ridolfi, Phys. Lett. **B378** (1996) 255.
- [6] T.K. Gehrman and W.J. Stirling, Phys. Rev. **D53** (1996) 6100.
- [7] E. Berger and J. Qiu, Phys. Rev. **D40** (1989) 778, 3128;  
 S. Gupta, D. Indumathi and M. Murthy, Z. Phys. **C42** (1989) 493; Erratum **C44** (1989) 356;  
 H.-Y. Cheng and S.-N. Lai, Phys. Rev. **D41** (1990) 91;  
 C. Bourrely, J.Ph. Guillet and J. Soffer, Nucl. Phys. **B361** (1991) 72;  
 P. Chiappetta, P. Colangelo, J.Ph. Guillet and G. Nardulli, Z. Phys. **C59** (1993) 629;  
 P. Mathews and R. Ramachandran, Z. Phys. **C53** (1992) 305;  
 S. Güllenstern, P. Gornicki, L. Mankiewicz and A. Schäfer, Phys. Rev. **D51** (1995) 3305.
- [8] A.P. Contogouris, B. Kamal, Z. Merebashvili and F.V. Tkachov, Phys. Lett. **B304** (1993) 329; Phys. Rev. **D48** (1993) 4092.
- [9] L.E. Gordon and W. Vogelsang, Phys. Rev. **D48** (1993) 3136.
- [10] L.E. Gordon and W. Vogelsang, Phys. Rev. **D49** (1994) 170.
- [11] P. Aurenche, R. Baier, M. Fontannaz, J.F. Owens and M. Werlen, Phys. Rev. **D39** (1989) 3275.
- [12] A.D. Martin, R.G. Roberts, W.J. Stirling, Phys. Lett. **B354** (1995) 155.
- [13] J. Huston et al., Phys. Rev. **D51** (1995) 6139.
- [14] W. Vogelsang and A. Vogt, Nucl. Phys. **B453** (1995) 334.
- [15] W.-D. Nowak, DESY 96-095, hep-ph/9605411.
- [16] RHIC Spin Collab., D. Hill et al., letter of intent RHIC-SPIN-LOI-1991;  
 G. Bunce et al., Particle World **3** (1992) 1.
- [17] M. Glück, E. Reya, and A. Vogt, Z. Phys. **C67** (1995) 433.

- [18] M. Stratmann and W. Vogelsang, DO-TH 96/10 and RAL-TR-96-033, hep-ph/9605330, to appear in Z. Phys. **C**.
- [19] P. Aurenche, R. Baier, M. Fontannaz and D. Schiff, Nucl. Phys. **B297** (1988) 661; H. Baer, J. Ohnemus and J.F. Owens, Phys. Lett. **B234** (1990) 127; Phys. Rev. **D42** (1990) 61.
- [20] F. Aversa, P. Chiappetta, M. Greco and J.Ph. Guillet, Phys. Lett. **B210** (1988) 225; Phys. Lett. **B211** (1988) 465; Nucl. Phys. **B327** (1989) 105.
- [21] M. Glück, E. Reya and A. Vogt, Phys. Rev. **D48** (1993) 116. Of the two LO,NLO sets presented in this work we choose those which have an additional hadronic component at the input scale.
- [22] J.G. Körner, D. Kreimer, and K. Schilcher, Z. Phys. **C54** (1992) 503.
- [23] G. 't Hooft and M. Veltman, Nucl. Phys. **B44** (1972) 189; P. Breitenlohner and D. Maison, Comm. Math. Phys. **52** (1977) 11.
- [24] J. Babcock, E. Monsay and D. Sivers, Phys. Rev. **D19** (1979) 1483.
- [25] P. Aurenche, P. Chiappetta, M. Fontannaz, J.Ph. Guillet and E. Pilon, Nucl. Phys. **B399** (1993) 34.
- [26] L.E. Gordon and W. Vogelsang, Phys. Rev. **D50** (1994) 1901.
- [27] M. Glück, L.E. Gordon, E. Reya and W. Vogelsang, Phys. Rev. Lett. **73** (1994) 388.

## Figure Captions

**Fig.1** Gluon distributions at  $Q^2 = 10 \text{ GeV}^2$  of the four NLO sets of polarized parton distributions used in this paper. The dotted line refers to set C of [6], whereas the other distributions are taken from [4] as described in the text. For comparison we also show the unpolarized NLO gluon distribution of [17].

**Fig.2 a:**  $p_T$ -dependence of the NLO polarized cross section for inclusive prompt photon production at HERA- $\vec{N}$  for the four sets of spin-dependent parton distributions. The results are presented at c.m.s. rapidity  $\eta = 0$ . The cross section for set C of [6] has been multiplied by  $-1$ . For comparison we also show the unpolarized NLO cross section. The scales have been chosen to be  $\mu_R = \mu_F = M_F = p_T/2$ . **b:** Asymmetries  $A_{LL}$  corresponding to **a** (here the result for set 'GS C' [6] is shown with its actual sign). The expected statistical errors indicated by the bars have been calculated according to Eq. (5) and as explained in the text. **c,d:** Same as **a,b**, but for the  $\eta$ -dependence at  $p_T = 6 \text{ GeV}$ .

**Fig.3 a:**  $p_T$ -dependence of the  $K$ -factors (as defined in Eq. (6)) for the unpolarized and the polarized cross sections at  $\eta = 0$ . The polarized results are shown for the three sets of parton distributions taken from [4] (see text); line drawings are as in Fig. 2. **b:** Comparison of the LO and NLO asymmetries  $A_{LL}$  for the three sets of polarized parton distributions taken from [4] (see text). The NLO curves are as already shown in Fig. 2b. **c,d:** Same as **a,b**, but for the  $\eta$ -dependence at  $p_T = 6 \text{ GeV}$ .

**Fig.4 a:**  $p_T$ -dependence of the ratios  $R$  (as defined in Eq. (7)) for the unpolarized and polarized cross sections at  $\eta = 0$ . The polarized results are shown for the three sets of parton distributions taken from [4] (see text); line drawings are as in Fig. 2. **b:** The scale dependence of the NLO asymmetries  $A_{LL}$  for the three sets of polarized parton distributions taken from [4] (see text). The curves for the scales  $\mu_R = \mu_F = M_F = p_T/2$  are as already shown in Fig. 2b and are displayed in the same line drawings. For each set the dotted (long-dashed) line corresponds to the scales  $p_T$  ( $2p_T$ ). **c,d:** Same as **a,b**, but for the  $\eta$ -dependence at  $p_T = 6 \text{ GeV}$ .

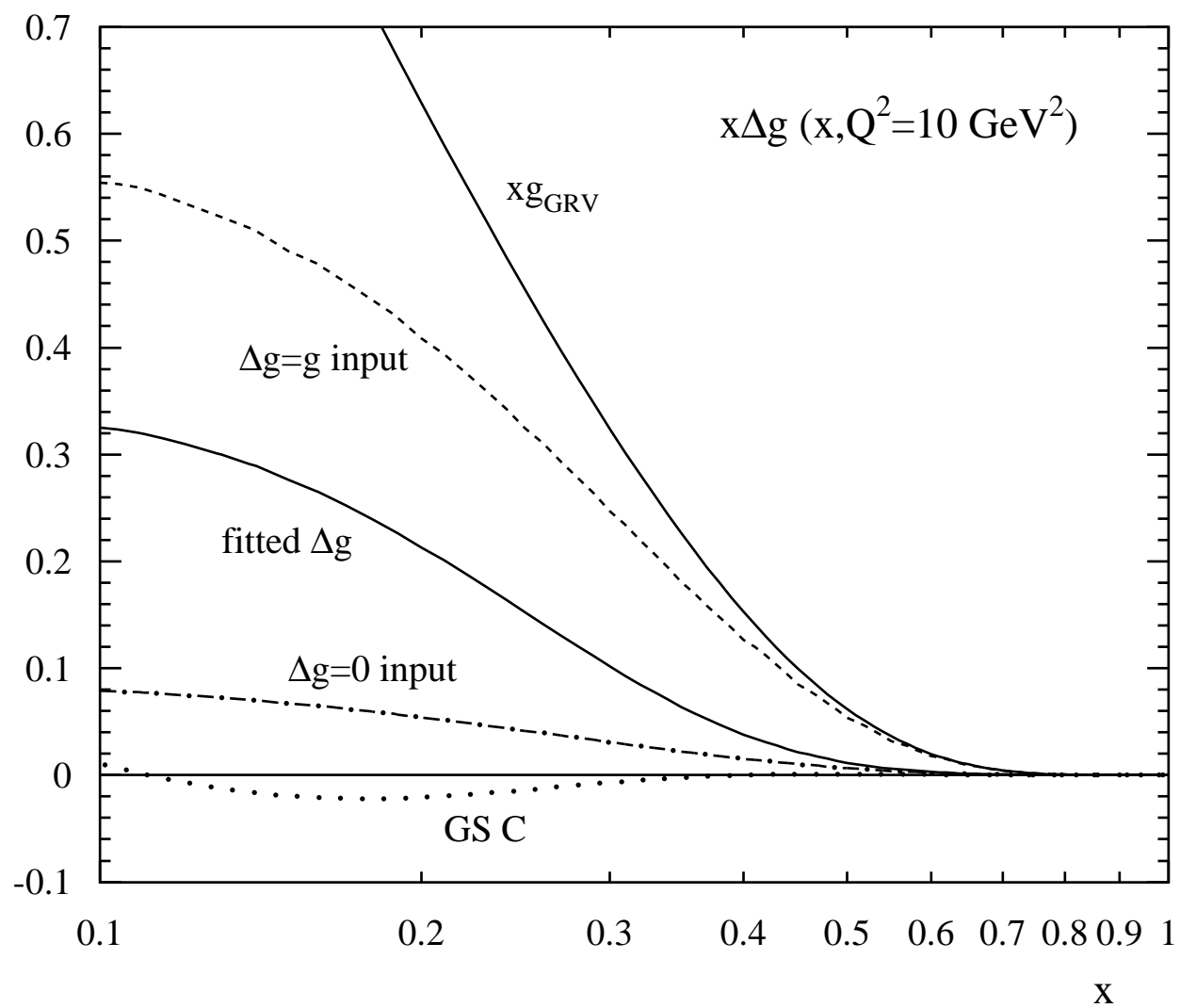


Fig. 1

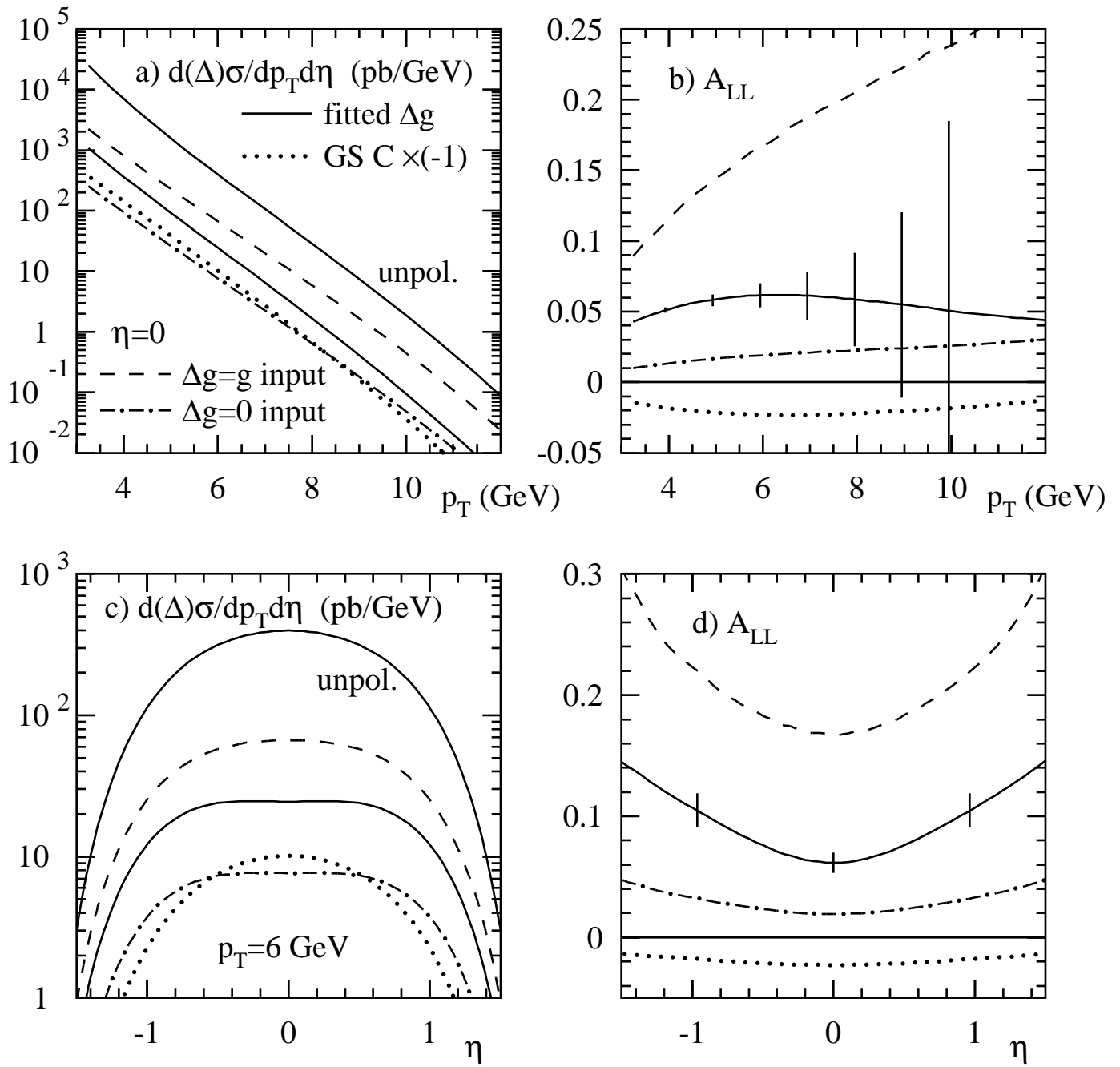


Fig. 2

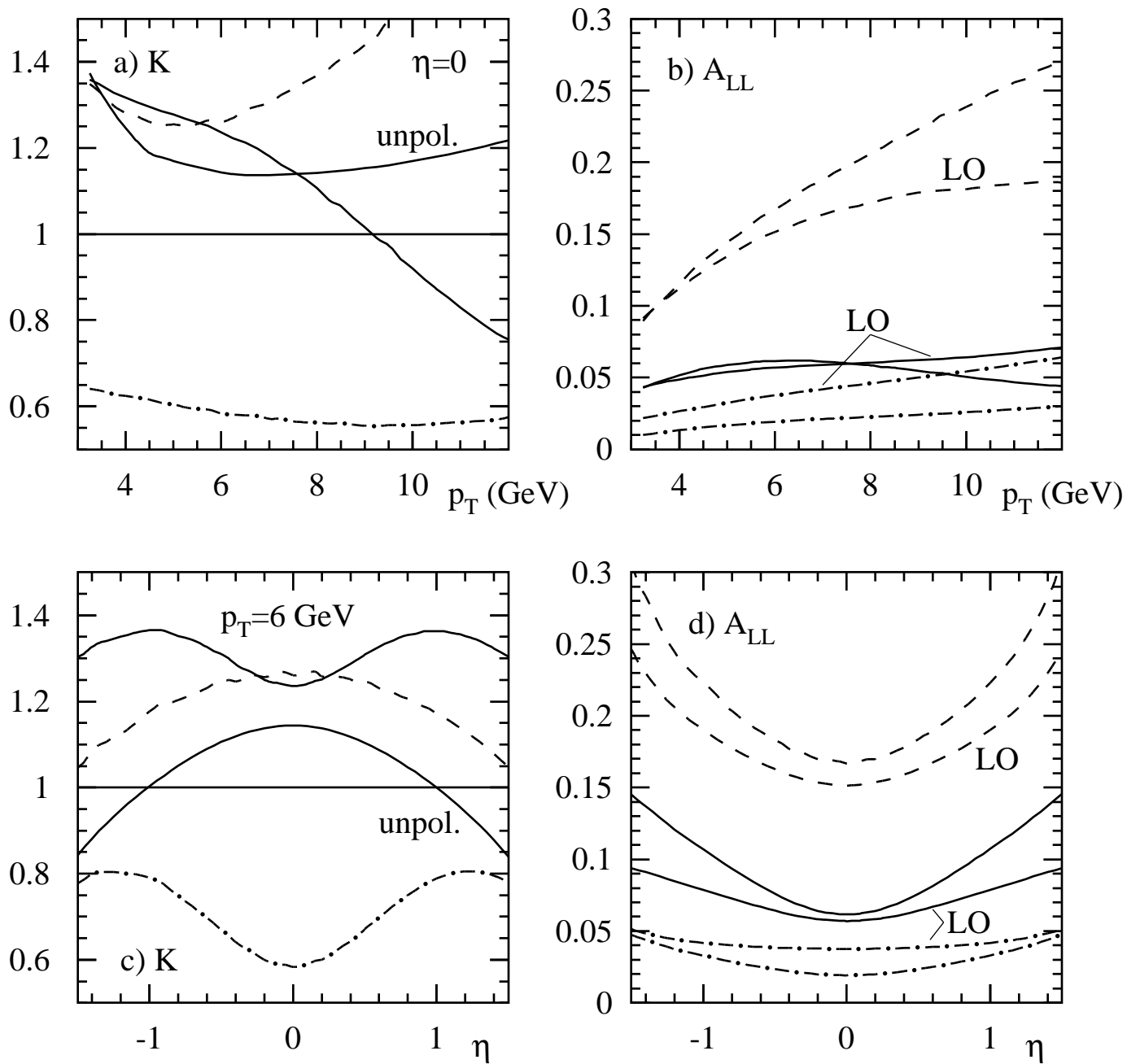


Fig. 3

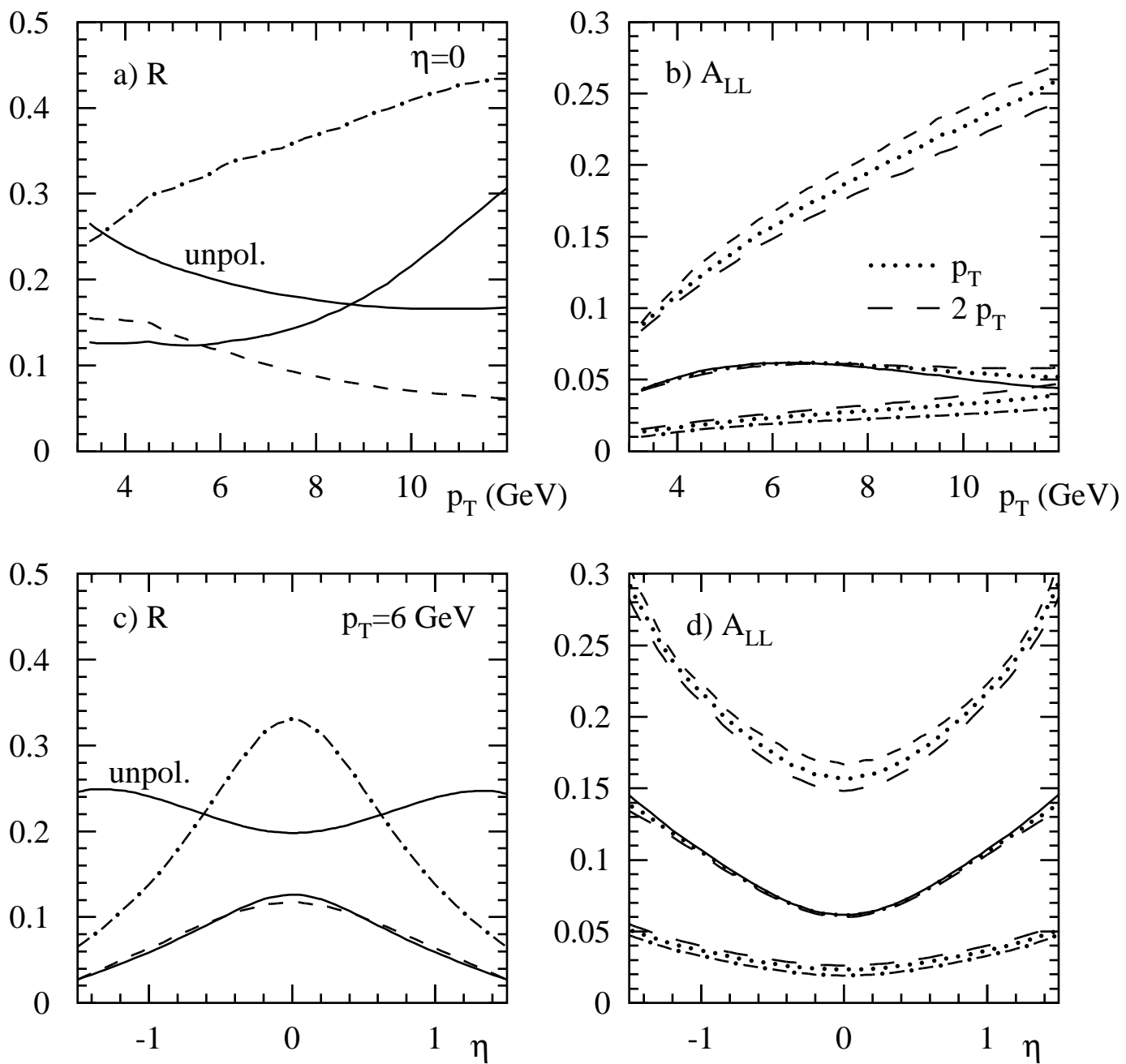


Fig. 4